

## Progress on Neutron-Target Multipoles above 1 GeV

I.I. Strakovsky<sup>1,a</sup>, W. Chen<sup>2</sup>, H. Gao<sup>2</sup>, W.J. Briscoe<sup>1</sup>, D. Dutta<sup>3</sup>, A.E. Kudryavtsev<sup>4</sup>, M. Mirazite<sup>5</sup>, M. Paris<sup>6</sup>, P. Rossi<sup>5</sup>, S. Stepanyan<sup>7</sup>, V.E. Tarasov<sup>4</sup>, and R.L. Workman<sup>1</sup>

<sup>1</sup> The George Washington University, Washington, DC 20052, USA

<sup>2</sup> Duke University, Durham, NC 27708, USA

<sup>3</sup> Mississippi State University, Mississippi State, MS 39762, USA

<sup>4</sup> Institute of Theoretical and Experimental Physics, Moscow, 117259 Russia

<sup>5</sup> INFN, Laboratori Nazionali di Frascati, 00044 Frascati, Italy

<sup>6</sup> Theory Division, Los Alamos National Laboratory, Los Alamos, NM 87545, USA

<sup>7</sup> Thomas Jefferson National Accelerator Facility, Newport News, VA 23606, USA

**Abstract.** We report a new extraction of nucleon resonance couplings using  $\pi^-$  photo-production cross sections on the neutron. The world database for the process  $\gamma n \rightarrow \pi^- p$  above 1 GeV has quadrupled with the addition of new differential cross sections from the CEBAF Large Acceptance Spectrometer (CLAS) at Jefferson Lab in Hall B. Differential cross sections from CLAS have been improved with a new final-state interaction determination using a diagrammatic technique taking into account the SAID phenomenological  $NN$  and  $\pi N$  final-state interaction amplitudes. Resonance couplings have been extracted and compared to previous determinations. With the addition of these new cross sections, significant changes are seen in the high-energy behavior of the SAID cross sections and amplitudes.

The GW group is focusing on the study of  $NN$  and  $\pi N$  elastic scattering as well as on the study of  $\gamma N \rightarrow \pi(\eta)N$  reactions. The former subject was devoted to study of electro-magnetic (EM) couplings  $N^*(\Delta^*) \rightarrow \gamma N$ . The radiative decay width of the neutral  $N^*$ - and  $\Delta^*$ -states may be extracted from  $\pi^-$  and  $\pi^0$  photoproduction on the neutron target (typically the deuteron) and requires the use of the model dependent nuclear corrections [final-state interaction (FSI)]. As a result, our knowledge of the neutral resonance decays is less precise compared to the charged ones.

For today, the experimental information on the reactions on the proton is more reach than that on the neutron (15%) [1]. Only with good data on both proton and neutron targets, one can hope to disentangle the isoscalar and isovector EM couplings of various  $N^*$  and  $\Delta^*$  resonances [2], as well as the isospin properties of the non-resonant background amplitudes.

Partially, it is compensated by experiments on pionic beams, e.g.,  $\pi^- p \rightarrow \gamma n$  (not  $\pi^0 n \rightarrow \gamma n$ ) as Crystal Ball Collaboration made, for instance, at BNL [3] for the inverse photon energy  $E_\gamma=285 - 689$  MeV and  $\theta=41 - 148^\circ$ . This process is free from complications associated with the deuteron target. However, the disadvantage of using the reaction  $\pi^- p \rightarrow \gamma n$  is the 5 to 500 times larger cross sections for  $\pi^- p \rightarrow \pi^0 n \rightarrow \gamma \gamma n$  depending on pion kinetic energy  $T_\pi$  and  $\gamma$  production angle  $\theta$ . That is why, we are forcing to use the deuteron as the neutron target.

In a further study of the FSI corrections for the  $\gamma n \rightarrow \pi^- p$  cross section determination from the deuteron data, we used a diagrammatic technique [4]. The Feynman diagrams corresponding to the Impulse Approximation (IA) [Fig. 1(a)] and  $pp$ -FSI [Fig. 1(b)], and  $\pi N$ -FSI [Fig. 1(c)] amplitudes for the reaction  $\gamma d \rightarrow \pi^- pp$  is shown in Fig. 1. IA and  $\pi N$ -FSI diagrams [Figs. 1(a),(c)] include also the cross-terms final protons.

<sup>a</sup> e-mail: igor@gwu.edu

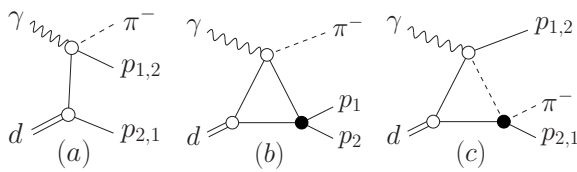


**Fig. 1.** Feynman diagrams for the leading components of the  $\gamma d \rightarrow \pi^- pp$  amplitude. (a) IA, (b)  $pp$ -FSI, and (c)  $\pi N$ -FSI. Filled black circles show FSI vertices. Wavy, dashed, solid, and double lines correspond to the photons, pions, nucleons, and deuterons, respectively.

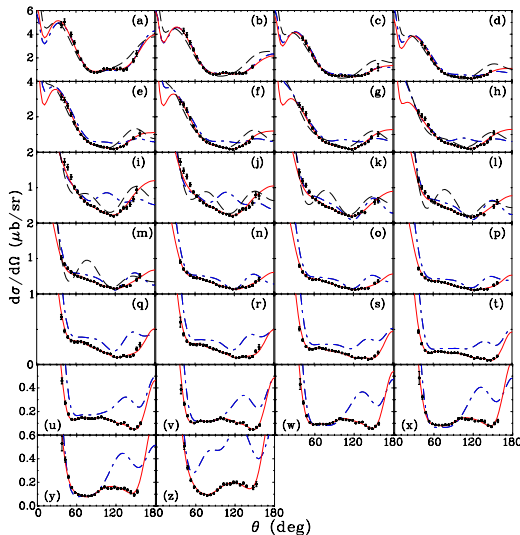


**Fig. 2.** The differential cross section for  $\gamma n \rightarrow \pi^- p$  below  $E_\gamma = 2.7$  GeV versus pion CM angle. Solid (dash-dotted) lines correspond to the GB12 (SN11 [12]) solution. Dashed lines give the MAID07 [14] predictions. Experimental data are from the current (filled circles). Plotted uncertainties are statistical. (a)  $E = 1050$  MeV, (b)  $E = 1100$  MeV, (c)  $E = 1150$  MeV, (d)  $E = 1200$  MeV, (e)  $E = 1250$  MeV, (f)  $E = 1300$  MeV, (g)  $E = 1350$  MeV, (h)  $E = 1400$  MeV, (i)  $E = 1450$  MeV, (j)  $E = 1500$  MeV, (k)  $E = 1550$  MeV, (l)  $E = 1600$  MeV, (m)  $E = 1650$  MeV, (n)  $E = 1700$  MeV, (o)  $E = 1750$  MeV, (p)  $E = 1800$  MeV, (q)  $E = 1850$  MeV, (r)  $E = 1900$  MeV, (s)  $E = 2000$  MeV, (t)  $E = 2100$  MeV, (u)  $E = 2200$  MeV, (v)  $E = 2300$  MeV, (w)  $E = 2400$  MeV, (x)  $E = 2500$  MeV, (y)  $E = 2600$  MeV, and (z)  $E = 2700$  MeV.

The  $\gamma N \rightarrow \pi N$  amplitudes were expressed through four independent Chew-Goldberger-Low-Nambu (CGLN) amplitudes [5], which were generated by the SAID code, using the GW DAC pion photoproduction multipoles [6]. The  $NN$ - and  $\pi N$ -scattering amplitudes were calculated, using the results of GW  $NN$  [7] and  $\pi N$  [8] PWAs. The DWF was taken from the Bonn potential (full model) [9]. The elementary amplitudes are dependent on the momenta of the external and intermediate particles in Fig. 1. Thus, Fermi motion is taken into account in the  $\gamma d \rightarrow \pi^- pp$  amplitude.

We applied FSI corrections [4] dependent on the  $E_\gamma$  and pion production  $\theta$  and taking into account a kinematical cut with momenta less (more) than  $200$  MeV/ $c$  for slow (fast) outgoing protons. Overall, the FSI correction factor  $R < 1$ , while the effect, i.e., the  $(1 - R)$  value, is less than 10% and the behavior is very smooth vs. pion production angle.

The contribution of FSI calculations [4] to the overall systematics is estimated to be 2% (3%) below (above)  $1800$  MeV. Then we added FSI systematics to the overall experimental systematics in quadrature.

We have included the new cross sections from the CLAS experiment [10] in a number of multipole analyses covering incident photon energies up to  $2.7$  GeV, using the full SAID database, in order to gauge the influence of these measurements, as well as their compatibility with previous measurements [11].

A comparison of the CLAS data with fits and predictions is given in Fig. 2. It is interesting to note that the data appear to have fewer angular structures than the earlier fits. The overall  $\chi^2$  has remained stable against the growing database, which has increased by a factor of 2 since 1995 (most of this increase comes from data from photon-tagging facilities).

In fitting the data, the stated experimental systematic uncertainties have been used as an overall normalization adjustment factor for the angular distributions [12]. Presently, the pion photoproduction database below  $E_\gamma = 2.7$  GeV consists of 26179 data points that have been fit in the GB12 (GZ12 [13]) solution with  $\chi^2 = 54832$  (50998). The contribution to the total  $\chi^2$  in the GB12 (GZ12) analyses of the 626 new CLAS  $\gamma n \rightarrow \pi^- p$  data points (e.g., those data points up to  $E_\gamma = 2.7$  GeV) is 1580 (1190). This should be compared to a starting  $\chi^2 = 45636$  for the new CLAS data using predictions from our previous SN11 solution [12].

## Progress on Neutron-Target Multipoles above 1 GeV

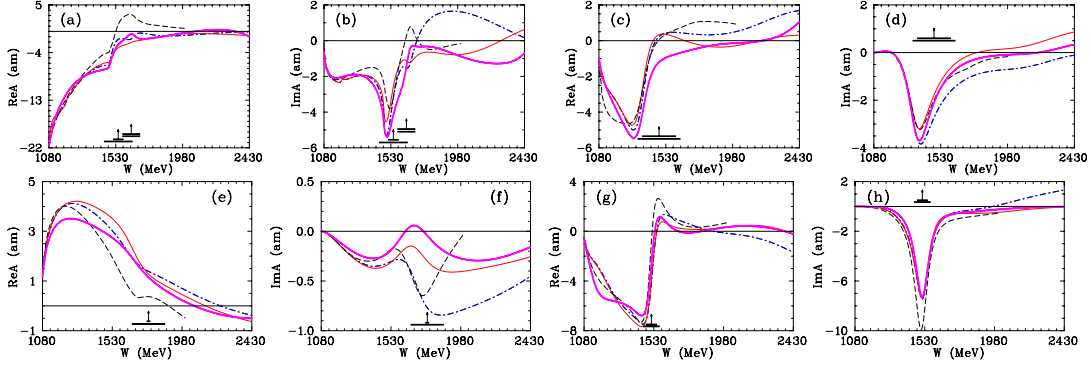


**Fig. 3.** Dominant neutron multipole  $I=1/2$  amplitudes from threshold to  $W = 2.43$  GeV ( $E_\gamma = 2.7$  GeV). Solid (dash-dotted) lines correspond to the GB12 (SN11 [12]) solution. Thick solid (dashed) lines give GZ12 solution (MAID07 [14], which terminates at  $W = 2$  GeV). (a)  $\text{Re}[{}_n E_{0+}^{1/2}]$ , (b)  $\text{Im}[{}_n E_{0+}^{1/2}]$ , (c)  $\text{Re}[{}_n M_{1-}^{1/2}]$ , (d)  $\text{Im}[{}_n M_{1-}^{1/2}]$ , (e)  $\text{Re}[{}_n M_{1+}^{1/2}]$ , (f)  $\text{Im}[{}_n M_{1+}^{1/2}]$ , (g)  $\text{Re}[{}_n E_{2-}^{1/2}]$ , and (h)  $\text{Im}[{}_n E_{2-}^{1/2}]$ . Vertical arrows indicate mass ( $W_R$ ), and horizontal bars show full ( $\Gamma$ ) and partial ( $\Gamma_{\pi N}$ ) widths of resonances extracted by the Breit-Wigner fit of the  $\pi N$  data associated with the SAID solution SP06 [8].

**Table 1.** Breit-Wigner resonance parameters [mass ( $W_R$ ), full ( $\Gamma$ ), and partial ( $\Gamma_{\pi N}$ ) widths of resonances] associated with the SAID solution SP06 [8] obtained from  $\pi N$  scattering (second column) and neutron helicity amplitudes  $A_{1/2}$  and  $A_{3/2}$  (in  $[(\text{GeV})^{-1/2} \times 10^{-3}]$  units) from the GB12 solution (first row), previous SN11 [12] solution (second row), and average values from the PDG10 [15] (third row).

Resonance	$\pi N$ SAID	$A_{1/2}$	$A_{3/2}$
$N(1535)1/2^-$	$W_R=1547$ MeV $\Gamma=188$ MeV $\Gamma_{\pi N}/\Gamma=0.36$	$-58\pm 6$ $-60\pm 3$ $-46\pm 27$	
$N(1650)1/2^-$	$W_R=1635$ MeV $\Gamma=115$ MeV $\Gamma_{\pi N}/\Gamma=1.00$	$-40\pm 10$ $-26\pm 8$ $-15\pm 21$	
$N(1440)1/2^+$	$W_R=1485$ MeV $\Gamma=284$ MeV $\Gamma_{\pi N}/\Gamma=0.79$	$48\pm 4$ $45\pm 15$ $40\pm 10$	
$N(1520)3/2^-$	$W_R=1515$ MeV $\Gamma=104$ MeV $\Gamma_{\pi N}/\Gamma=0.63$	$-46\pm 6$ $-47\pm 2$ $-59\pm 9$	$-115\pm 5$ $-125\pm 2$ $-139\pm 11$
$N(1675)5/2^-$	$W_R=1674$ MeV $\Gamma=147$ MeV $\Gamma_{\pi N}/\Gamma=0.39$	$-58\pm 2$ $-42\pm 2$ $-43\pm 12$	$-80\pm 5$ $-60\pm 2$ $-58\pm 13$
$N(1680)5/2^+$	$W_R=1680$ MeV $\Gamma=128$ MeV $\Gamma_{\pi N}/\Gamma=0.70$	$26\pm 4$ $50\pm 4$ $29\pm 10$	$-29\pm 2$ $-47\pm 2$ $-33\pm 9$

Resonance couplings were extracted as in Ref. [12], are listed in Table 1 and compared to the previous SN11 determinations and the Particle Data Group (PDG) averages [15]. Couplings for the  $N(1440)1/2^+$ ,  $N(1520)3/2^-$ , and  $N(1675)5/2^-$  are reasonably close to the SN11 estimates. The value of  $A_{1/2}$  found for the  $N(1535)1/2^-$ , using the GB12 fit, is very close to the SN11 determination. Using the GZ12 fit, however, the result is somewhat larger in magnitude ( $-85 \pm 15$ ). A similar feature was found for the proton couplings, using this form, in Ref. [13]. Using this alternate form, a determination of the  $N(1650)1/2^-$   $A_{1/2}$  was difficult and resulted in a value, lower in magnitude by about 50%. For this reason, we consider the uncertainty associated with this state to be a lower limit only. No value was quoted for the  $N(1720)3/2^+$  state. As can be seen in Figs. 3, the two different fit forms GB12 and GZ12, though similar in shape, have opposite signs for the imaginary parts of corresponding

multipoles ( ${}_nE_{1+}^{1/2}$  and  ${}_nM_{1+}^{1/2}$ ) in the neighborhood of the resonance position, and even the sign can not be determined. This is in line with the PDG estimates, which also fail to give signs for the couplings to this state.

Let us **summarize**: a comprehensive set of differential cross section at 26 energies for negative-pion photoproduction on the neutron, via the reaction  $\gamma d \rightarrow \pi^- pp$ , have been determined with a JLab tagged-photon beam for incident photon energies from 1.05 to 2.7 GeV. To accomplish a state-of-the-art analysis, we included new FSI corrections using a diagrammatic technique, taking into account a kinematical cut with momenta less (more) than 200 MeV/c for slow (fast) outgoing protons.

The updated PWAs examined mainly the effect of new CLAS neutron-target data on the SAID multipoles and resonance parameters. These new data have been included in a SAID multipole analysis, resulting in new SAID solutions, GB12 and GZ12. A major accomplishment of this CLAS experiment is a substantial improvement in the  $\pi^-$ -photoproduction database, adding 626 new differential cross sections, quadrupling the world database for  $\gamma n \rightarrow \pi^- p$  above 1 GeV. Comparison to earlier SAID fits, and a lower-energy fit from the Mainz group, shows that the new solutions are much more satisfactory at higher energies.

On the experimental side, further improvements in the PWAs await more data, specifically in the region above 1 GeV, where the number of measurements for this reaction is small. Of particular importance in all energy regions is the need for data obtained involving polarized photons and polarized targets. Due to the closing of hadron facilities, new  $\pi^- p \rightarrow \gamma n$  experiments are not planned and only  $\gamma n \rightarrow \pi^- p$  measurements are possible at electromagnetic facilities using deuterium targets. Our agreement with existing  $\pi^-$  photoproduction measurements leads us to believe that these photoproduction measurements are reliable despite the necessity of using a deuterium target. We hope that new CLAS  $\Sigma$ -beam asymmetry measurements for  $\gamma n \rightarrow \pi^- p$ , at  $E_\gamma = 910$  up to 2400 MeV will soon [16] provide further constraints for the neutron multipoles.

Obviously, any meson photoproduction treatment on the “neutron” target requires a FSI study. Generally, FSI depends on the full set of kinematical variables of the reaction. In our analysis, the FSI correction factor depends on the photon energy, meson production angle, and is averaged on the rest of variables in the region of “quasi-free” process on the neutron.

The authors acknowledge helpful comments and preliminary fits from R. A. Arndt in the early stages of this work. We acknowledge the outstanding efforts of the CLAS Collaboration who made the experiment possible. This work was supported in part by the U.S. Department of Energy Grants, by the Russian, by the Russian Atomic Energy Corporation, the National Science Foundation, and the Italian Istituto Nazionale di Fisica Nucleare.

## References

1. W. J. Briscoe, I. I. Strakovsky, and R. L. Workman, Institute of Nuclear Studies of The George Washington University Database; [http://gwdac.phys.gwu.edu/analysis/pr\\_analysis.html](http://gwdac.phys.gwu.edu/analysis/pr_analysis.html) .
2. K. M. Watson, Phys. Rev. **95** (1954) 228; R. L. Walker, Phys. Rev. **182** (1969) 1729.
3. A. Shafi, *et al.* (Crystal Ball Collaboration), Phys. Rev. C **70**, 035204 (2004).
4. V. E. Tarasov *et al.*, Phys. Ref. C **84**, (2011) 035203.
5. G. F. Chew, M. L. Goldberger, F. E. Low, and Y. Nambu, Phys. Rev. **106**, 1345 (1957).
6. M. Dugger (CLAS Collaboration), Phys. Rev. C **76**, 025211 (2007).
7. R. A. Arndt, *et al.*, Phys. Rev. C **76**, (2007) 025211.
8. R. A. Arndt, *et al.*, Phys. Rev. C **74**, (2006) 045205.
9. R. Machleidt, *et al.*, Phys. Rept. **140**, (1987) 1.
10. W. Chen *et al.*, (CLAS Collaboration), Phys. Rev. Lett. **103**, (2009) 012301.
11. W. Chen, *et al.*, Phys. Rev. C **86**, 015206 (2012).
12. R. L. Workman, *et al.*, Phys. Rev. C **85**, 025201 (2012).
13. R. L. Workman, *et al.*, Phys. Rev. C **86**, 015202 (2012).
14. D. Drechsel, *et al.*, Eur. Phys. J. A **34**, 69 (2007).
15. K. Nakamura *et al.* (Particle Data Group), J. Phys. G **37**, 075021 (2010).
16. D. Sokhan, Ph.D. Thesis, Edinburgh University, 2009.